Nearly touching spheres in a viscoelastic fluid

Rajat Dandekar[1] and Arezoo M. Ardekani[1]
School of Mechanical Engineering, Purdue University, West Lafayette, IN 49707, USA

(*Electronic mail: rabhiji@purdue.edu)

(Dated: 31 August 2021)

We theoretically investigate the forces and moments acting on two nearly touching spheres immersed in a second-order fluid. We divide the problem into four sub-classes, where each class represents the translational or rotational motion of the spheres either along the line joining the centers or the axis which is oriented perpendicular to the line joining the centers. Using a regular perturbation solution methodology with the Deborah number as the small parameter, we obtain analytical expressions for the hydrodynamic forces and the moments experienced by the spheres for each sub-class considered. We find that, while the introduction of viscoelasticity does not generate any torques on the spheres, the viscoelastic contribution to force is non-zero and acts along the line joining the sphere centers for each sub-class. For asymmetric sub-classes, the presence of viscoelasticity produces a lift force on the spheres. We validate our method with the reciprocal theorem approach and find our force estimates to be accurate for small sphere separations. The analytical expressions obtained in this study can be utilized in computational schemes to study the behavior of a suspension of particles immersed in a viscoelastic fluid.

I. INTRODUCTION

Suspension of particles are encountered in many industrial applications, biological processes and consumables. In such systems, particles are generally immersed in a fluid medium which can exhibit complex rheological behavior such as shear rate dependent solvent viscosity, viscoelasticity or a combination of both. Even a marginal deviation of the solvent from a Newtonian behavior has been shown to affect the dynamics of the suspended particles in non-trivial ways[1] and has been exploited for several particle manipulation and control applications[2–5]. Towards successfully predicting the behavior of a suspension of interacting particles immersed in a complex fluid, understanding the binary interactions of particles forms a fundamental building block which demands attention. In this study, we focus upon the hydrodynamic interaction between two spherical particles suspended in a viscoelastic fluid with a shear rate independent viscosity.

For understanding the binary interaction of spheres in a homogeneous fluid, four classes of problems are studied in the literature: i) Spheres translating along the line joining their centers, ii) Spheres rotating along the line joining their centers, iii) Spheres rotating perpendicular to the line joining their centers and iv) Spheres translating perpendicular to the line joining their centers. Figure 1 shows a schematic representation of such problems. The theoretical analysis considering the motion of two spheres in a Newtonian fluid for these classes of problems has received considerable attention in the literature and several important contributions spanning several decades have helped us dissect the problem in great detail. We list some of the important contributions here. Stimson and Jeffery[6] studied the motion of two spheres moving along the line joining their centers in the same direction and evaluated the force acting on the spheres for arbitrary sphere separations. Using a similar theoretical framework, Brenner and Maude[7,8] extended their analysis for spheres approaching each other along the common axis . Jeffery[9] analyzed the problem considering two spheres rotating about their common axis and evaluated the torques acting on the spheres. Later, a comprehensive theoretical analysis of the asymmetrical motion of two spheres was also performed[10]. Although the above studies provided an analysis which was valid for arbitrary sphere separations, asymptotic solutions when the spheres were close to each other were considered valuable which led to focused efforts in that direction. Cooley and O'Neill[11] first used a method of matched asymptotic expansion to obtain an expression for the force acting on two close spheres translating in the same direction. They divided the domain of analysis into an inner region (neighborhood of the nearest points on the spheres) and the outer region (rest of the domain) and performed a matching analysis between the solutions obtained in both regions. Similar methodology involving matched asymptotic expansions was used by Hansford[12] to determine an expression for the force acting on two equal spheres which are approaching each other. The leading order force term scales as ε^{-1} in both the cases studied by Cooley and O'Neill and Hansford[11,12], where $\varepsilon \ll 1$ denotes the non-dimensional distance between spheres. In their work, Cooley and O'Neill also noticed that, instead of obtaining the solutions in both the inner and outer regions, the solution obtained in the gap between the spheres is sufficient to obtain the singular terms in the force expression. Using this insight, Jeffrey[13] extended the calculation by Hansford for unequal spheres by using a lubrication theory approach and calculated the force upto an order of $\varepsilon \log \varepsilon$. Similar derivations using lubrication theory in the inner region exist for asymmetric motions of the spheres for small sphere gaps[14,15]. The above mentioned works are displayed in a tabular form in Table Ia.

The contributions related to nearly touching spheres in a Newtonian fluid have proved invaluable as researchers have utilized the analytical expressions in computational schemes involving a suspension of spheres such as Stokesian Dynamics, where computational tractability is of vital importance. The asymptotic expressions for the forces is a useful alternative to mesh refinement procedures for small particle separations while evaluating the properties of a suspension of particles immersed in a fluid[13].

For viscoelastic fluids, theoretical studies include under-

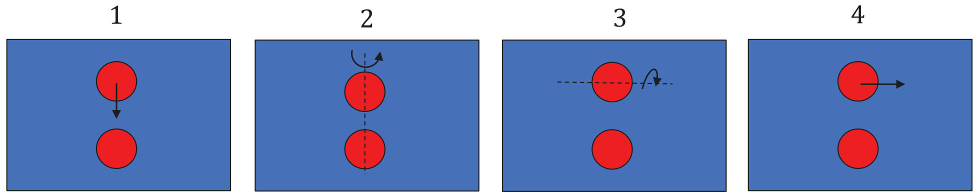

FIG. 1. Different types of problems involving binary interaction of spheres.

standing the flow past a sphere immersed in a fluid with weak viscoelasticity and negligible inertia[16–18]. These studies however considered an unbounded fluid and neglected any wall effects. Later the influence of bounded domain was taken into account, where initially weak wall effects were considered[19–21]. Subsequently, several theoretical and numerical studies have focused on particles near a plane wall[22–25]. In comparison with Newtonian fluids, there are limited theoretical studies involving interaction of particles in a viscoelastic fluid. Brunn[26] represented the viscoelastic fluid using a second-order fluid model and considered the sedimentation of two spheres for large sphere separations. They found that the distance between the sphere centers decreases for spheres sedimenting in a quiescent fluid with their velocity vectors directed along or perpendicular to the line joining their centers. Ardekani, Rangel, and Joseph[27] studied the motion two spheres suspended in a free stream of second-order fluid and evaluated the forces acting on the spheres for arbitrary sphere separations. In their study, by assuming that, $\alpha_1 + \alpha_2 = 0$, where α_1 and α_2 are fluid parameters related to first and second normal stress coefficients, they predicted the trajectories of the two spheres for axisymmetric as well as asymmetric motions. Phillips developed a procedure to evaluate the forces acting on N spheres suspended in a second-order fluid for small Deborah numbers[28]. However, they provided expressions in the form of integrals which is computationally expensive and not straightforward to include in simulations involving a suspension of spheres. Khair and Squires[29] proposed a methodology to measure normal stress coefficients of a second-order fluid by using reciprocal theorem to calculate the relative force acting between the spheres for spheres translating parallel and perpendicular to their line of centers. Biviscous fluid model is also employed to study the lubrication forces between nearly touching particles in complex fluids[30,31]. Such models are useful to predict the suspension rheology for shear-thinning and shear-thickening fluids.

Lubrication theory is applicable for a fluid moving through a narrow gap between two solid boundaries. Such theories find application in the mechanical design of bearings to determine the oil pressure distribution inside the bearing. These lubricants are often classified as viscoelastic due to the addition of polymers. Consequently, significant theoretical and experimental progress has been made to understand the performance of viscoelastic lubricants as compared to lubricants with Newtonian properties. Several models have been used to model the non-Newtonian properties such as the power-law model[32], Rabinowitsch model[33], pseudo-plastic model[34], upper convective Maxwell's model[35], Phan-Thien-Tanner model[36] and the Oldroyd-B model[37] (please refer to the introduction of Abbaspur *et al.*[38], for a detailed review on this topic). The results of these studies are however, catered to fluid moving through a bearing (journal or sliding), where the boundaries are assumed to be flat surfaces. Application of viscoelastic forces to enable propulsion of swimmers, even at low Deborah numbers has received increasing attention recently. For such applications, the use of analytical force and torque expressions for co-rotating and counter-rotating spheres immersed in a viscoelastic fluid are useful for predicting the swimming speed and understanding the swimming mechanism[39–41]. To the best of our knowledge, there has not been a systematic study to understand the viscoelastic forces and torques acting on nearly touching spheres, for all four types of problems outlined in figure 1 (refer to Table Ib). Towards aiding simulations of a suspension of interacting spheres and developing a theoretical framework, such an analysis is important and would complement numerical schemes used to understand rheology of spheres immersed in viscoelastic fluids[42–46]. In this work, we study the motion of two nearly touching spheres in a viscoelastic fluid for the four cases described in figure 1: i) Unequal spheres translating along the line joining their centers, ii) Unequal spheres rotating about the line joining their centers, iii) Unequal spheres rotating about the axis perpendicular to the line joining their centers, and iv) Unequal spheres translating along the axis perpendicular to the line joining their centers. Following the approach commonly employed for binary interaction of spheres in a Newtonian fluid, we are prescribing the velocities on the surface of the spheres and determining the hydrodynamic forces and the torques acting on the spheres. We model the fluid viscoelasticity using a second-order fluid model. Such a model has been employed extensively in the literature and is useful to include the effect of weak fluid elasticity in the absence on any shear thinning effects[28]. The analysis presented in this manuscript is valid for weakly viscoelastic fluids with small Deborah numbers ($\sim 10^{-2} - 10^{-3}$). For problem type 1, we use two different approaches to solve the forces/torques experienced by the spheres and show that both the approaches lead to the same result for small sphere separations. The first approach consists of solving the equations of motion explicitly in the gap between the spheres and then evaluating the analytical expres-

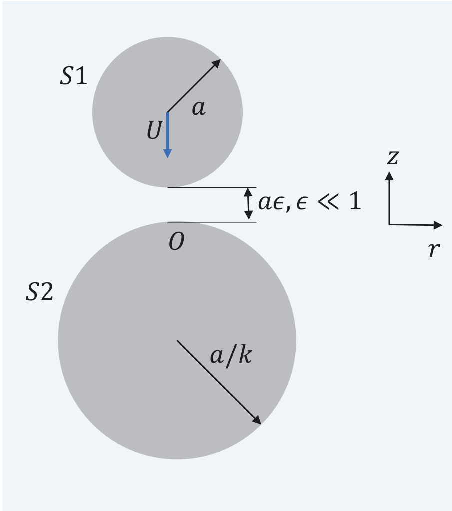

FIG. 2. Spheres immersed in a second-order fluid, with sphere $S1$ approaching the stationary sphere $S2$ with velocity U. The separation between the spheres is εa, where $\varepsilon \ll 1$.

sions for forces/torques by integrating the stress tensor on the surface of the particle. The second approach consists of using a reciprocal theorem framework, which bypasses the fluid flow calculations and the contribution of the fluid elasticity to the force/torque is represented in the form of an integral equation. The purpose of solving the problem with two different approaches is to provide a validation for the lubrication theory solution for viscoelastic fluids and confirm that the outer solution does not contribute to the forces and torques experienced by the spheres. Subsequently, for problem types 2, 3 and 4, we only use the first approach to evaluate the forces and moments experienced by the spheres.

II. PROBLEM FORMULATION (TYPE 1)

Figure 2 shows a schematic representation of the type 1 problem. The radius of sphere $S1$ is a, while that of sphere $S2$ is a/k. Such a radius choice ensures that substituting $k=0$ allows us to obtain insights for sphere near a plane wall as well. Previous research works highlighted in the introduction have used the notation of $-a/k$ for the radius of sphere $S2$, where $k<0$. To avoid any confusion in the sign while interpreting the results, we consider the radius of sphere $S2$ as a/k, where $k>0$. The sphere $S1$ is approaching with a velocity U towards sphere $S2$ which is stationary. Both the spheres are immersed in a second-order fluid with fluid viscosity μ. The origin $O(z=0, r=0)$ is located on the surface of the stationary sphere at the closest point of the gap as shown in the figure. The spheres are separated by a distance of εa, where $\varepsilon \ll 1$. We have assumed the fluid inertia to be negligible in our analysis. Consequently, the momentum and mass conservation equations for a second-order fluid are given as follows,

$$\nabla \cdot \boldsymbol{T} = \boldsymbol{0}, \quad \nabla \cdot \boldsymbol{u} = 0. \tag{1}$$

Here, $\boldsymbol{u}$ denotes the fluid velocity and $\boldsymbol{T}$ denotes the stress tensor in the fluid which is given by[27],

$$\boldsymbol{T} = -p\boldsymbol{I} + \mu\dot{\boldsymbol{\gamma}}_{(1)} + \alpha_1\dot{\boldsymbol{\gamma}}_{(2)} + \alpha_2\dot{\boldsymbol{\gamma}}_{(1)}^2. \tag{2}$$

We obtain the above equation by conducting a retarded motion expansion of the stress tensor. $\dot{\boldsymbol{\gamma}}_{(1)}$ denotes the rate-of-strain tensor and $\dot{\boldsymbol{\gamma}}_{(2)}$ denotes the first convected derivative of the rate-of-strain tensor. Here p is the fluid pressure, μ is the zero shear fluid viscosity, $\alpha_1 = -\frac{\psi_1}{2}$ and $\alpha_2 = \psi_1 + \psi_2$, where ψ_1, ψ_2 are the first and second normal stress coefficients, respectively. Note that, $\alpha_1 < 0$ and α_2 can either be positive or negative[47]. The tensors $\dot{\boldsymbol{\gamma}}_{(1)}$ and $\dot{\boldsymbol{\gamma}}_{(2)}$ are defined as,

$$\dot{\boldsymbol{\gamma}}_{(1)} = \nabla\boldsymbol{u} + \nabla\boldsymbol{u}^T, \tag{3}$$

$$\dot{\boldsymbol{\gamma}}_{(2)} = \frac{\partial \dot{\boldsymbol{\gamma}}_{(1)}}{\partial t} + \boldsymbol{u}\cdot\nabla\dot{\boldsymbol{\gamma}}_{(1)} + \dot{\boldsymbol{\gamma}}_{(1)}\cdot\nabla\boldsymbol{u} + \nabla\boldsymbol{u}^T\cdot\dot{\boldsymbol{\gamma}}_{(1)}. \tag{4}$$

We non-dimensionalize the governing equations of motion using the following scales: length scale $l_c = a$, velocity scale $u_c = U$, pressure scale $p_c = \mu U/a$. Henceforth, we use the same variables to denote the dimensionless variables. The non-dimensional form of the stress tensor can be expressed as follows,

$$\boldsymbol{T} = -p\boldsymbol{I} + \dot{\boldsymbol{\gamma}}_{(1)} - De\left(\dot{\boldsymbol{\gamma}}_{(2)} + B_{11}\dot{\boldsymbol{\gamma}}_{(1)}^2\right). \tag{5}$$

Here, $De = -\alpha_1 U/a\mu$ is the Deborah number which signifies the ratio between the relaxation time scale $(-\alpha_1/\mu)$ and the flow time scale (a/U), and $B_{11} = \alpha_2/\alpha_1$. The positive value of the Deborah number is ensured as the value of α_1 is generally found to be negative[47]. The values of B_{11} lie between -1 and 1. As the Type 1 problem is axisymmetric, we expect that the velocity and the pressure fields do not vary in the azimuthal direction. The velocity field can thus be written as, $\boldsymbol{u} = (u_r, 0, u_z)$. We express the velocity components in terms of the stream function as follows,

$$u_r = -\frac{1}{r}\frac{\partial \psi}{\partial z}, \quad u_z = \frac{1}{r}\frac{\partial \psi}{\partial r}. \tag{6}$$

We now define stretched coordinates in the gap between the spheres as follows[13,15],

$$R = r/\varepsilon^{1/2}, \quad Z = z/\varepsilon.$$

In this coordinate system, the surface of the moving sphere (S_1) is represented as $Z = H_1 = 1 + R^2/2 + O(\varepsilon)$ and the surface of the stationary sphere is represented as $Z = H_2 = -kR^2/2 + O(\varepsilon)$. We shall be working in this stretched coordinate system for the following portion of the manuscript.

A. Solution

We use a regular perturbation scheme with the Deborah number (De) as the small parameter and express the velocity

	Work	Problem Type	Method	Distance
(*a*)	Stimson and Jeffery[6]	1	Bipolar coordinates	Arbitrary
	Maude[8]	1 (approaching)	Bipolar coordinates	Arbitrary
	Jeffery[9]	2	Bipolar coordinates	Arbitrary
	O'Neill and Majumdar[10]	3,4	Bipolar coordinates	Arbitrary
	Cooley and O'Neill[11]	1	Matched asymptotics	small
	Hansford[12]	1 (approaching)	Matched asymptotics	small
	Jeffrey[13]	1	Lubrication theory	small
	O'Neill and Majumdar[14]	3,4	Lubrication theory	small
	Jeffrey and Onishi[15]	2,3,4 (approaching)	Lubrication theory	small
	Work	**Problem Type**	**Method**	**Distance**
(*b*)	Brunn[26]	1	Regular perturbation	large
	Phillips, Khair and Squires[28,29]	2,4	Reciprocal Theorem	Arbitrary
	Ardekani, Rangel, and Joseph[27]	1,2,3,4 (free stream)	$\alpha_1+\alpha_2=0$	Arbitrary
	Our work	1,2,3,4	Lubrication Theory	small

TABLE I. Summary of previous theoretical works for binary interaction of spheres in (*a*) Newtonian fluid and (*b*) Viscoelastic (second-order) fluid (refer to figure 1 for a visual representation of the problem types).

and the pressure fields as a summation in terms of successive powers of De as follows,

$$\boldsymbol{u} = \boldsymbol{u}^{(0)} + De\boldsymbol{u}^{(1)} + O(De^2), \quad p = p^{(0)} + Dep^{(1)} + O(De^2). \tag{7}$$

Consequently, the stress tensor can be expressed as $\boldsymbol{T} = \boldsymbol{T}^{(0)} + De\boldsymbol{T}^{(1)} + O(De^2)$ where,

$$\boldsymbol{T}^{(0)} = -p^{(0)}\boldsymbol{I} + \dot{\boldsymbol{\gamma}}^{(0)}_{(1)},$$
$$\boldsymbol{T}^{(1)} = -p^{(1)}\boldsymbol{I} + \dot{\boldsymbol{\gamma}}^{(1)}_{(1)} - (\dot{\boldsymbol{\gamma}}^{(0)}_{(2)} + B_{11}\dot{\boldsymbol{\gamma}}^{(0)}_{(1)} \cdot \dot{\boldsymbol{\gamma}}^{(0)}_{(1)}). \tag{8}$$

Here, it is important to note that, for the perturbation analysis to be valid, the Deborah number based on the leading order velocity in the gap and the separation between the spheres (denoted by De_h) , should be small. Since $u_r^{(0)} \sim U\varepsilon^{-1/2}$, this condition can be expressed as follows,

$$De_h = De\varepsilon^{-3/2} \ll 1. \tag{9}$$

The above equation can be used to determine the relative magnitudes of De and ε for which our analysis is valid. For typical range of $\varepsilon \sim 10^{-1} - 10^{-2}$, we find that our analysis is valid for weakly viscoelastic fluids with $De \ll 10^{-2} - 10^{-3}$. We now solve the governing equations of motion (refer to equations (1)) at successive orders of De.

1. *Solution at* $O(1)$

The leading order governing equation of motion is given by,

$$-\nabla p^{(0)} + \nabla^2 \boldsymbol{u}^{(0)} = \boldsymbol{0}. \tag{10}$$

The boundary conditions at the leading order are given by,

$$\boldsymbol{u}(Z = H_1) = -\hat{\boldsymbol{e}}_z, \quad \boldsymbol{u}(Z = H_2) = \boldsymbol{0}. \tag{11}$$

The leading order solution which satisfies the boundary conditions is obtained by conducting a perturbation analysis with the small parameter as the minimum gap between the spheres denoted by ε (detailed solution can be found in Jeffrey[13]). The leading order stream function is thus expressed as,

$$\psi^{(0)} = \varepsilon\psi_0^{(0)} + \varepsilon^2\psi_1^{(0)} + \varepsilon^3\psi_2^{(0)} + O(\varepsilon^4). \tag{12}$$

For sake of completeness, expressions for $\psi_0^{(0)}$, $\psi_1^{(0)}$ and $\psi_2^{(0)}$ are provided in Appendix A.

2. *Solution at* $O(De)$

The equations of motion at the first order in Deborah number are given by,

$$-\nabla p^{(1)} + \nabla^2 \boldsymbol{u}^{(1)} = \nabla \cdot (\dot{\boldsymbol{\gamma}}^{(0)}_{(2)} + B_{11}\dot{\boldsymbol{\gamma}}^{(0)}_{(1)} \cdot \dot{\boldsymbol{\gamma}}^{(0)}_{(1)}). \tag{13}$$

The boundary conditions at the first order are given by,

$$\boldsymbol{u}^{(1)}(Z = H_1) = \boldsymbol{0}, \quad \boldsymbol{u}^{(1)}(Z = H_2) = \boldsymbol{0}. \tag{14}$$

We represent the first order stream function as a perturbation expansion series with ε as the small parameter. The stream function is thus written as,

$$\psi^{(1)} = \psi_0^{(1)} + \varepsilon\psi_1^{(1)} + \varepsilon^2\psi_2^{(1)} + O(\varepsilon^3). \tag{15}$$

The first order pressure field can be expressed as,

$$p^{(1)} = \varepsilon^{-3}p_0^{(1)} + \varepsilon^{-2}p_1^{(1)} + \varepsilon^{-1}p_2^{(1)} + O(1). \tag{16}$$

The pressure scaling of ε^{-3} is driven by the magnitude of the terms on the right-hand side of equation (13). Substituting the series expansions for the stream function and the pressure in equation (13), we obtain governing equations for the pressure and the stream function at each successive order which will be described in detail in the next subsections.

Solution for $\psi_0^{(1)}, p_0^{(1)}$

We write the governing equations and the boundary conditions at the leading order in ε as follows,

$$-\frac{\partial p_0^{(1)}}{\partial R}+\frac{\partial^3\psi_0^{(1)}}{\partial Z^3}=H\left(\nabla\cdot(\dot{\gamma}_{(2)}^{(0)}+B_{11}\dot{\gamma}_{(1)}^{(0)}\cdot\dot{\gamma}_{(1)}^{(0)})\cdot\hat{e}_r,-7/2\right), \tag{17}$$

$$-\frac{\partial p_0^{(1)}}{\partial Z}=H\left(\nabla\cdot(\dot{\gamma}_{(2)}^{(0)}+B_{11}\dot{\gamma}_{(1)}^{(0)}\cdot\dot{\gamma}_{(1)}^{(0)})\cdot\hat{e}_z,-4\right). \tag{18}$$

Here, $H(f,n)$ denotes the coefficient of ε^n in the expression for f. The above equations are subjected to the following boundary conditions,

$$\psi_0^{(1)}=0,\quad \frac{\partial\psi_0^{(1)}}{\partial Z}=0\quad \text{at } Z=H_1, \tag{19}$$

$$\psi_0^{(1)}=0,\quad \frac{\partial\psi_0^{(1)}}{\partial Z}=0\quad \text{at } Z=H_2. \tag{20}$$

After solving the above equations of motion, we obtain the following expressions for the leading order stream function and the pressure.

$$\psi_0^{(1)}=\frac{1}{5(-2+(k-1)R^2)^6}(6(1+B_{11})R^2 \times(2+(k+1)R^2-4Z)(2+R^2-2Z)^2(kR^2-2Z)^2), \tag{21}$$

$$p_0^{(1)}=-\frac{1}{5(-2+(k-1)R^2)^6}72(2(4+(-7-19k+19k^2+7k^3)R^6)-2((k-1)R^4(-27-53k+80Z+80kZ) +8(k-1)R^2(3-20Z+20Z^2))+B_{11}(8+(-9-13k+13k^2+9k^3)R^6-2(k-1)R^4(-17-23k+40Z+40kZ)) +B_{11}(4(k-1)R^2(7-40Z+40Z^2))). \tag{22}$$

Solution for $\psi_1^{(1)}, p_1^{(1)}$

The equations of motion and the boundary conditions at $O(\varepsilon)$ are given by,

$$\frac{\partial p_1^{(1)}}{\partial R}+\frac{\partial^3\psi_1^{(1)}}{\partial Z^3}+\frac{\partial}{\partial R}\left(\frac{1}{R}\frac{\partial^2\psi_0^{(1)}}{\partial R\partial Z}\right)= H\left(\nabla\cdot(\dot{\gamma}_{(2)}^{(0)}+B_{11}\dot{\gamma}_{(1)}^{(0)}\cdot\dot{\gamma}_{(1)}^{(0)})\cdot\hat{e}_r,-5/2\right), \tag{23}$$

$$-\frac{\partial p_1^{(1)}}{\partial Z}-\frac{1}{R}\frac{\partial^3\psi_0^{(1)}}{\partial R\partial Z^2}=H\left(\nabla\cdot(\dot{\gamma}_{(2)}^{(0)}+B_{11}\dot{\gamma}_{(1)}^{(0)}\cdot\dot{\gamma}_{(1)}^{(0)})\cdot\hat{e}_z,-3\right). \tag{24}$$

The above equations are subjected to the following boundary conditions,

$$\psi_1^{(1)}=0,\quad \frac{\partial\psi_1^{(1)}}{\partial Z}=-\frac{R^4}{8}\frac{\partial^2\psi_0^{(1)}}{\partial Z^2}\quad \text{at } Z=H_1, \tag{25}$$

$$\psi_1^{(1)}=0,\quad \frac{\partial\psi_1^{(1)}}{\partial Z}=-k^3\frac{R^4}{8}\frac{\partial^2\psi_0^{(1)}}{\partial Z^2}\quad \text{at } Z=H_2. \tag{26}$$

We solve the above set of equations using the *Wolfram Mathematica* software and detailed expressions for $\psi_1^{(1)}, p_1^{(1)}$ are not provided here for the sake of brevity. This solution can be found in the Supplementary Material.

Solution for $\psi_2^{(1)}, p_2^{(1)}$

The equations of motion and the boundary conditions at $O(\varepsilon^2)$ are given by,

$$-\frac{\partial p_2^{(1)}}{\partial R}+\frac{\partial^3\psi_2^{(1)}}{\partial Z^3}+\frac{\partial}{\partial R}\left(\frac{1}{R}\frac{\partial^2\psi_1^{(1)}}{\partial R\partial Z}\right)= H\left(\nabla\cdot(\dot{\gamma}_{(2)}^{(0)}+B_{11}\dot{\gamma}_{(1)}^{(0)}\cdot\dot{\gamma}_{(1)}^{(0)})\cdot\hat{e}_r,-3/2\right), \tag{27}$$

$$-\frac{\partial p_2^{(1)}}{\partial Z}-\frac{1}{R}\frac{\partial^3\psi_1^{(1)}}{\partial R\partial Z^2}-\frac{1}{R}\frac{\partial}{\partial R}\left(R\frac{\partial}{\partial R}\left(\frac{1}{R}\frac{\partial\psi_0^{(1)}}{\partial R}\right)\right)= H\left(\nabla\cdot(\dot{\gamma}_{(2)}^{(0)}+B_{11}\dot{\gamma}_{(1)}^{(0)}\cdot\dot{\gamma}_{(1)}^{(0)})\cdot\hat{e}_z,-2\right). \tag{28}$$

The above equations are subjected to the following boundary conditions,

$$\psi_2^{(1)}=\frac{R^8}{128}\frac{\partial\psi_0^{(1)}}{\partial Z^2},\quad \frac{\partial\psi_2^{(1)}}{\partial Z}=-\frac{R^4}{8}\frac{\partial^2\psi_1^{(1)}}{\partial Z^2} -\frac{R^6}{16}\frac{\partial^2\psi_0^{(1)}}{\partial Z^2}-\frac{R^8}{128}\frac{\partial^3\psi_0^{(1)}}{\partial Z^3}\quad \text{at } Z=H_1, \tag{29}$$

$$\psi_2^{(1)}=k^6\frac{R^8}{128}\frac{\partial\psi_1^{(1)}}{\partial Z^2},\quad \frac{\partial\psi_2^{(1)}}{\partial Z}=-k^3\frac{R^4}{8}\frac{\partial^2\psi_1^{(1)}}{\partial Z^2} -k^5\frac{R^6}{16}\frac{\partial^2\psi_0^{(1)}}{\partial Z^2}-k^6\frac{R^8}{128}\frac{\partial^3\psi_0^{(1)}}{\partial Z^3}\quad \text{at } Z=H_2. \tag{30}$$

Again, due to the lengthy form of the solutions, detailed expressions for $\psi_2^{(1)}, p_2^{(1)}$ are not provided here for the sake of brevity. Note that, the solutions at all orders were verified by substituting the expressions obtained back in the governing equations of motion. Having obtained the velocity and pressure fields in the vicinity of the spheres, we can conduct an integration of these variables on the surface of the spheres to evaluate the hydrodynamic force and torque experienced by the spheres which is explained in the next section.

B. Hydrodynamic force and torque experienced by the spheres

The hydrodynamic force and the torque experienced by the spheres are non-dimensionalized with the scales ($F_c = 6\pi\mu u_c a$) and ($G_c = 8\pi\mu u_c a^2$), respectively, and can be written as a series expansion with Deborah number (De) as the small parameter as follows,

$$\boldsymbol{F}_i = \boldsymbol{F}_i^{(0)} + De\boldsymbol{F}_i^{(1)} + O(De^2), \tag{31}$$

$$\boldsymbol{G}_i = \boldsymbol{G}_i^{(0)} + De\boldsymbol{G}_i^{(1)} + O(De^2). \tag{32}$$

Here, $i = 1,2$ denotes spheres $S1$ and $S2$, respectively. The expressions for the leading order force and torque experienced by the spheres are provided by[13] as follows,

$$\boldsymbol{F}_i^{(0)} = \pm\left(\frac{1}{\varepsilon(1+k)^2} - \frac{1+7k+k^2}{5(1+k)^3}\log\varepsilon - \frac{1+18k-29k^2+18k^3+k^4}{21(1+k)^4}\varepsilon\log\varepsilon + O(1)\right)\hat{\boldsymbol{e}}_z. \tag{33}$$

$$\boldsymbol{G}_i^{(0)} = \boldsymbol{0}. \tag{34}$$

The $\pm$ sign signifies the equal and opposite repulsive forces acting on both the spheres. We can obtain the viscoelastic contribution to the force and torque by substituting the velocity and pressure fields in the first order stress tensor (refer to $\boldsymbol{T}^{(1)}$ in equation (8)) and evaluating the following integrals on the surface of the sphere,

$$\boldsymbol{F}_i^{(1)} = \int_{S_i}\left(\boldsymbol{T}^{(1)}\cdot\boldsymbol{n}\right)dS, \tag{35}$$

$$\boldsymbol{G}_i^{(1)} = \int_{S_i}\left(\boldsymbol{r}\times\boldsymbol{T}^{(1)}\cdot\boldsymbol{n}\right)dS. \tag{36}$$

Here $\boldsymbol{n}$ is the unit normal vector on the surface of the sphere and $\boldsymbol{r}$ is the vector oriented from the sphere center to the surface of the sphere. We evaluate the above integrals and obtain the following expressions for the first order force and torque experienced by the spheres,

$$\boldsymbol{F}_i^{(1)} = \pm\left(\frac{3\pi(8+3B_{11})}{5(1+k)^2\varepsilon^2} + \frac{K(k,B_{11})}{\varepsilon} + L(k,B_{11})\frac{\log\varepsilon}{\varepsilon}\right)\boldsymbol{e}_z, \tag{37}$$

$$\boldsymbol{G}_i^{(1)} = \boldsymbol{0}. \tag{38}$$

Here,

$$K(k,B_{11}) = \frac{3(k+1)^3(143+8k+B_{11}(8k+98))}{350(k+1)^4}, \tag{39}$$

and

$$L(k,B_{11}) = 3(4B_{11}(k+1)^2(13k^2-19k+13) + 5(14k^4-5k^3+4k^2-5k+14))/(350(k+1)^3). \tag{40}$$

Note that, the leading order viscoelastic force contribution scales as De/ε^2 and acts along the line joining the centre of the spheres. Since the type 1 problem is axisymmetric, we expect that the first order hydrodynamic torque exerted on the spheres is zero as seen from equation (38). The contribution of viscoelasticity to the hydrodynamic stress tensor is given by $\boldsymbol{T}^{(1)}$, which is expressed as $\boldsymbol{T}^{(1)} = -p^{(1)}\boldsymbol{I} + \dot{\gamma}_{(1)}^{(1)} - (\dot{\gamma}_{(2)}^{(0)} + B_{11}\dot{\gamma}_{(1)}^{(0)}\cdot\dot{\gamma}_{(1)}^{(0)})$. We can extract the leading order contribution to the first order viscoelastic force acting in the $z-$direction by evaluating the expression $\hat{\boldsymbol{e}}_z\cdot\boldsymbol{T}^{(1)}\cdot\hat{\boldsymbol{e}}_z$ on the surface of either spheres. The individual terms contributing to the viscoelastic force can be associated with a first order pressure component $p^{(1)}$, first order viscous stress component $\dot{\gamma}_{(1)zz}^{(1)} = \hat{\boldsymbol{e}}_z\cdot\dot{\gamma}_{(1)}^{(1)}\cdot\hat{\boldsymbol{e}}_z$, and the polymeric stress component $\boldsymbol{Q}_{zz} = \hat{\boldsymbol{e}}_z\cdot(\dot{\gamma}_{(2)}^{(0)} + B_{11}\dot{\gamma}_{(1)}^{(0)}\cdot\dot{\gamma}_{(1)}^{(0)})\cdot\hat{\boldsymbol{e}}_z$. We now calculate the order of magnitude for each term in the force expression with an intention to elucidate the key contributions to the viscoelastic force and obtain the following,

$$p^{(1)} \sim \varepsilon^{-3}, \quad \dot{\gamma}_{(1)zz}^{(1)} \sim \varepsilon^{-2}\frac{1}{R}\frac{\partial^2\psi_0^{(0)}}{\partial Z^2}$$
$$\boldsymbol{Q}_{zz} \sim \varepsilon^{-3}(2+B_{11})\frac{1}{R^2}\left(\frac{\partial^2\psi_0^{(1)}}{\partial Z^2}\right)^2 \tag{41}$$

From the above analysis, we find that the first order pressure and the polymeric stress component vary with the gap between the spheres as ε^{-3}, while the first order viscous stress component varies as ε^{-2}. This indicates that the leading order viscoelastic force contribution is only from the first order pressure and the polymeric stress component and not the first order viscous stress component. Additionally, the order of magnitude analysis of the polymeric stress component reveals that it is the variation of the leading order radial velocity in

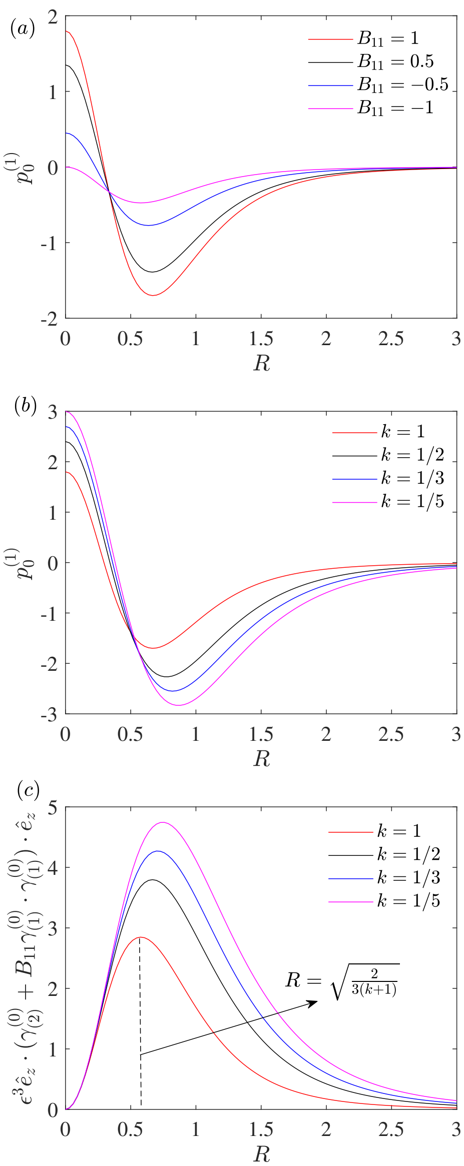

FIG. 3. a) Variation of the leading contribution to the first order pressure with the radial coordinate R for different values of B_{11}, b) Variation of the leading contribution to the first order pressure with the radial coordinate R for different values of k and c) Variation of the leading contribution to the polymeric stress component (denoted by $\boldsymbol{Q}_{zz}$ in the manuscript) with the radial coordinate R for different values of k for the type 1 problem.

the gap between the spheres which is the dominant part of this component. We also note that, both the first order pressure and the polymeric stress component vary linearly with B_{11} (refer to equations (22) and (41))which is manifested in the force expression as well (refer to equation (37)).

Since the first order pressure and the polymeric stress in the gap between the spheres are responsible for the leading order viscoelastic force, we focus on the spatial variation of these parameters on the surface of sphere $S1$. From figure 3a, we observe that the first order pressure is maximum at the point on the sphere surface which lies on the common axis of the spheres. The pressure further decreases and reaches a minimum at a radial distance $\sim 0.5 - 1\varepsilon^{1/2}a$ before attaining values close to zero. Figure 3b shows the influence of the radius difference in the spheres on the first order pressure distribution. We infer that the radius of the spheres influenced by their spherical geometry has a significant influence on the pressure, which implies that considering the spheres as flat surfaces for obtaining lubrication forces approximates would result in inaccurate force estimates. More precisely, we find that increasing the size of sphere $S2$ (decreasing value of k), increases the magnitude of first order pressure distribution in the gap between the spheres. Interestingly, the polymeric stress plotted in figure 3c reaches a maximum at radial distances greater than $R = 0$, with the radial location for the maximum polymeric stress increasing with increasing size of the sphere $S2$. The polymeric stress responsible for the type 1 viscoelastic force can be expressed in a simplified form as follows,

$$\boldsymbol{Q}_{zz} \sim \varepsilon^{-3}(2 + B_{11})\frac{2R}{((k+1)R^2+2)^4}. \tag{42}$$

The radial distance at which the polymeric stress attains maximum can be evaluated by solving the equation, $\frac{\partial \boldsymbol{Q}_{zz}}{\partial R} = 0$. We find that $R = \sqrt{\frac{2}{3(k+1)}}$, corresponds to the radial distance at which the polymeric stress is maximum. As the size of sphere $S2$ increases (decreasing value of k) and consequently the polydispersity of the system increases, the polymeric stress increases in magnitude as noticed from equation (42) and the radial location for the maximum polymeric stress moves further away from the common axis of the spheres. From figure 3a and equation (42), we also infer that increasing the value of B_{11} increases the magnitude of the pressure maximum, pressure minimum and the polymeric stress in the gap between the spheres.

For a sphere approaching a wall in a second-order fluid, we find the force by substituting $k = 0$ to be as follows,

$$\boldsymbol{F}_{wall}^{(1)} \sim \frac{3\pi(8 + 3B_{11})}{5\varepsilon^2}\boldsymbol{e}_z. \tag{43}$$

For viscoelastic fluids, $-1 < B_{11} < 1$. Consequently, from equation (37), we infer that the direction of the leading order viscoelastic force for sphere $S1$ is in the positive $z-$ direction which indicates a repulsive force. Table II shows the value of B_{11} and the corresponding viscoelastic force contribution for different viscoelastic models used in the literature[47]. As noted in equation (9), the results of this study are valid if the condition, $De \ll \varepsilon^{3/2}$ is satisfied. This limits the utility of this study in practice. However, there are practical scenarios where the results of this study are valid. In numerical simulation schemes such as Stokesian Dynamics, it is common to apply a hard core repulsion potential between the spheres, for radial distances larger than the hydrodynamic radius of the spheres. This becomes pertinent for systems with charge stabilization such as charged colloids, where the repulsion forces emerge from the overlap of the electric double layers. Another example concerns rough colloidal particles, where the particle roughness places a lower limit on the interparticle separation.

Model	B_{11}	DeF_1^1
FENE Dumbbells	0	$\frac{24\pi}{20}\frac{De}{\varepsilon^2}$
Multibead rod ($N=2$)	-0.28	$\frac{21.48\pi}{20}\frac{De}{\varepsilon^2}$
Multibead rod ($N=6$)	0.016	$\frac{24.5\pi}{20}\frac{De}{\varepsilon^2}$
Multibead rod ($N=70$)	0.17	$\frac{25.5\pi}{20}\frac{De}{\varepsilon^2}$
Bead-rod chain polymer melt	0.34	$\frac{27\pi}{20}\frac{De}{\varepsilon^2}$

TABLE II. Comparison of leading order viscoelastic force magnitude for different viscoelastic fluid models[47], for spheres of equal sizes ($k=1$).

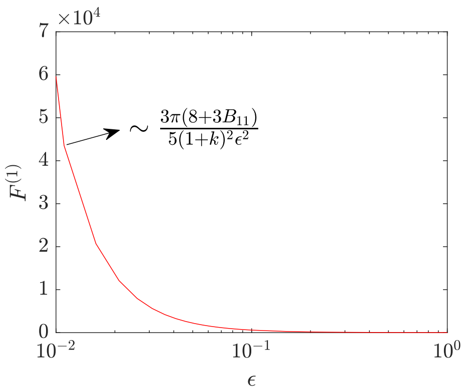

FIG. 4. First order non-dimensional force acting on the sphere $S1$ as a function of the separation distance between the spheres, evaluated using the reciprocal theorem approach.

In such examples, the radial distance is restricted from assuming values lower than a specific value due to constraints imposed by the system. The results of this study are valid for such examples and can be used to study the dynamics of interacting particles placed in a viscoelastic fluid. Additionally, we note that, the viscoelastic force expressions obtained in this study can provide an alternative repulsive term for non-colloidal spheres immersed in weakly viscoelastic matrices with potential applications in computational methods used to predict the shear rheology of suspensions. For example, the hydrodynamic force expression obtained for the type 1 problem can be used to model the interparticle repulsive forces which are essential in discontinuous shear thickening (DST) model of Newtonian suspensions. The effect of this residual viscoelasticity can become important at very low separations.

C. Reciprocal theorem approach

Here, we use the Lorentz reciprocal theorem to determine the first order force acting on the sphere $S1$. This method involves the calculation of the desired integrated quantities without requiring the full description of primary variables such as velocity and pressure[48]. Hence, by applying the reciprocal theorem for our problem, the knowledge of the flow field induced by two approaching spheres in a Newtonian fluid will be sufficient to determine the first order viscoelastic contribution to the force and torque. By comparing the results obtained from this approach, we seek to validate the method outlined in the previous sections. For applying the reciprocal theorem, we choose the auxillary problem to be that of sphere $S1$ moving towards the stationary sphere $S2$ in a Newtonian fluid. The solution of this problem is given by Brenner[7]. After applying the reciprocal theorem, we obtain the following integral expressions for the first order force acting on sphere $S1$ (derivation is provided in Appendix A).

$$\boldsymbol{F}_1 = \int_{V_f} \left(\boldsymbol{B}^{(0)} + B_{11} \boldsymbol{A}^{(0)} \cdot \boldsymbol{A}^{(0)} \right) : \nabla \boldsymbol{u}^{(0)} \hat{\boldsymbol{e}}_z. \tag{44}$$

Here, $\boldsymbol{u}^{(0)}$ denotes the fluid velocity field for two approaching spheres in a Newtonian fluid as given by Brenner[7] and V_f is the fluid volume enclosed by the two spheres. We note that the above expression can be used to evaluate the force acting on spheres with arbitrary separation. We substitute the velocity field and evaluate the above integral in a bispherical coordinate system, similar to the one used in Brenner[7]. Figure 4 shows the variation of the first order viscoelastic contribution to the force with the spheres separation. Table III shows a comparison between the force acting on the spheres by the two methods described in the manuscript for various values of the separation distance between the spheres for spheres of same sizes and spheres of unequal sizes with the radius differing by a factor of 2. We observe that the lubrication theory provides better estimates as the separation between the spheres reduces, as expected. For spheres separated less than 0.001 times the sphere radius, the error is less than 0.001% for spheres of equal sizes, while it is less than 0.06% for spheres of unequal sizes. We thus conclude that the lubrication theory provides accurate force estimates and the results of our work can be used to support computer simulations dedicated to solving problems involving interaction of multiple spheres immersed in a viscoelastic fluid. The lubrication method utilized in this study assumes that for small sphere gaps, only the flow field within the thin gap between the spheres (i.e, the inner solution) contributes to the hydrodynamic forces. The reciprocal theorem approach, however, considers the contribution of the entire fluid bounded by the spheres (i.e, the inner and outer solutions). Hence, this validation also confirms that, for a non-Newtonian fluid with weak viscoelasticity and small separation between the spheres, only the inner solution contributes to the viscoelastic force and the outer solution contribution can be neglected. Here, we note that, even if the outer solution does not contribute to the hydrodynamic forces and torques, the contribution of the outer solution to the flow field might be useful for other physical applications, such as propulsion of swimmers immersed in a viscoelastic fluid at low Deborah numbers[39].

III. PROBLEM FORMULATION (TYPE 2)

Figure 5 shows sphere $S1$ rotating with an angular velocity Ω about the line joining the centers of both the spheres and sphere $S2$ stationary. We use the same variables as before to denote the radius of the spheres and the distance between the spheres. We note that, the governing equations for this

	ε	Lubrication	Reciprocal	error %		ε	Lubrication	Reciprocal	error %
	0.5	5.667	7.049	24.3		0.5	9.00	8.57	4.7
	0.1	96.25	101.425	5.3		0.1	165.74	161.22	2.72
(*a*)	0.05	359.154	365.958	1.89	(*b*)	0.05	627.75	616.15	1.8
	0.01	8414.91	8425.51	0.12		0.01	14906	14817.6	0.5
	0.005	33346.3	33358.5	0.03		0.005	59174.6	58975.4	0.3
	0.001	826923	826939	0.001		0.001	1469000	1468000	0.06

TABLE III. Comparison of the vertical force $|\boldsymbol{F}^{(1)}|/2\pi$ acting on the spheres by two different methods for the type 1 problem (using lubrication theory and using reciprocal theorem) for(a) spheres of equal sizes ($k=1$) and (b) spheres of unequal sizes ($k=1/2$).

problem are the same as that of the type 1 problem (refer to equations (1)). We use the velocity scale $u_c = \Omega a$ to non-dimensionalize the equations of motion. We solve the equations of motion in the stretched coordinates (R,Z) as demonstrated for the type 1 problem.

A. Solution

Here, we again use the regular perturbation scheme to express the velocity and the pressure fields in terms of the Deborah number as follows,

$$\boldsymbol{u} = \boldsymbol{u}^{(0)} + De\boldsymbol{u}^{(1)} + O(De^2), \quad p = p^{(0)} + Dep^{(1)} + O(De^2). \tag{45}$$

We now proceed in a manner similar to the one adopted for the type 1 problem and solve for the velocity and pressure fields upto the first order in De.

1. Solution at $O(1)$

The leading order governing equation of motion is given by,

$$-\nabla p^{(0)} + \nabla^2 \boldsymbol{u}^{(0)} = \boldsymbol{0}. \tag{46}$$

The boundary conditions at the leading order are as follows,

$$\boldsymbol{u}(Z=H_1) = \hat{\boldsymbol{e}}_z \times \boldsymbol{r}, \quad \boldsymbol{u}(Z=H_2) = \boldsymbol{0}. \tag{47}$$

Here, $\boldsymbol{r}$ is the position vector from the center of the sphere to the sphere surface. The leading order solution which satisfies the boundary conditions is obtained by using a lubrication theory approach for $\varepsilon \ll 1$ as follows[15],

$$\boldsymbol{u}^{(0)} = \varepsilon^{1/2}\left(RZ - kR^3/2\right)(H_1 - H_2)^{-1}\hat{\boldsymbol{e}}_\theta. \tag{48}$$

2. Solution at $O(De)$

The equations of motion at the first order in Deborah number are given as follows,

$$-\nabla p^{(1)} + \nabla^2 \boldsymbol{u}^{(1)} = \nabla\cdot(\dot{\boldsymbol{\gamma}}^{(0)}_{(2)} + B_{11}\dot{\boldsymbol{\gamma}}^{(0)}_{(1)}\cdot\dot{\boldsymbol{\gamma}}^{(0)}_{(1)}). \tag{49}$$

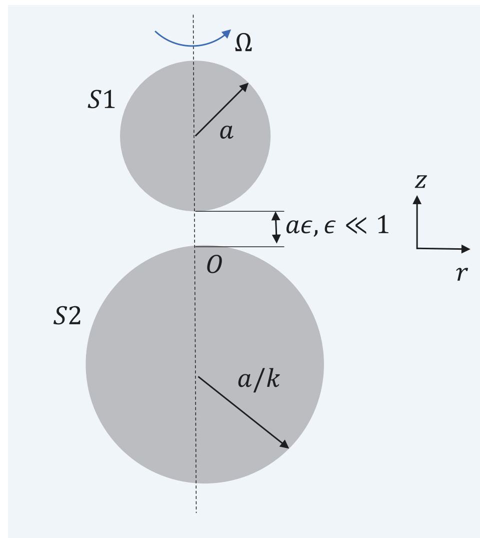

FIG. 5. Spheres immersed in a second-order fluid, with sphere $S1$ rotating with an angular velocity $\Omega\hat{\boldsymbol{e}}_z$ and sphere $S2$ stationary

The tensors $\dot{\boldsymbol{\gamma}}_{(1)}, \dot{\boldsymbol{\gamma}}_{(2)}$ are obtained by substituting the leading order solution described in equation (48). The boundary conditions are given by,

$$\boldsymbol{u}^{(1)}(Z=H_1) = \boldsymbol{0}, \quad \boldsymbol{u}^{(1)}(Z=H_2) = \boldsymbol{0}. \tag{50}$$

After substituting the leading order solution in equation (49), we find that the surface stresses have components only in the radial and the vertical directions which causes the azimuthal component of the first order velocity to be zero. Hence, due to the expected azimuthal symmetry of the first order flow, we can express the velocity field in terms of the stream function (refer to equation (6)). We express the stream function and the pressure as a perturbation expansion series in ε as follows,

$$\psi^{(1)} = \varepsilon^3\psi_0^{(1)} + O(\varepsilon^4) \tag{51}$$

$$p^{(1)} = \varepsilon^{-1}p_0^{(1)} + O(1). \tag{52}$$

Solution for $\psi_0^{(1)}, p_0^{(1)}$

We write the governing equations and the boundary conditions at the leading order in ε as follows,

$$-\frac{\partial p_0^{(1)}}{\partial R}+\frac{\partial^3 \psi_0^{(1)}}{\partial Z^3}=H\left(\nabla\cdot(\dot{\gamma}_{(2)}^{(0)}+B_{11}\dot{\gamma}_{(1)}^{(0)}\cdot\dot{\gamma}_{(1)}^{(0)})\cdot\hat{e}_r,-1/2\right), \tag{53}$$

$$-\frac{\partial p_0^{(1)}}{\partial Z}=H\left(\nabla\cdot(\dot{\gamma}_{(2)}^{(0)}+B_{11}\dot{\gamma}_{(1)}^{(0)}\cdot\dot{\gamma}_{(1)}^{(0)})\cdot\hat{e}_z,-1\right). \tag{54}$$

As mentioned previously, $H(f,n)$ denotes the coefficient of ε^n in the expression for f. The above equations are subjected to the following boundary conditions,

$$\psi_0^{(1)}=0,\quad \frac{\partial \psi_0^{(1)}}{\partial Z}=0 \quad \text{at } Z=H_1. \tag{55}$$

$$\psi_0^{(1)}=0,\quad \frac{\partial \psi_0^{(1)}}{\partial Z}=0 \quad \text{at } Z=H_2. \tag{56}$$

We solve the above equations and obtain the expressions for the stream function and the pressure for the Type 2 problem are obtained as follows,

$$\begin{aligned}\psi_0^{(1)}=&-\frac{1}{60)(-2+(k-1)R^2)^5}R^2(2+R^2-2Z)^2(kR^2-2Z)^2k^4R^6+k^2R^2(R^2(8-3Z)-14(Z-1))\\&+2B_{11}(-4-4(k-1)R^2+(k-1)^2R^4)(-2-R^2+k^2R^2+k(Z-3)-Z)+k^3R^4(Z-2R^2-12)\\&-(R^4+14R^2-8)(2+R^2+Z)+k(44+2R^6-8Z+R^4(20+3Z)+R^2(6+28Z))),\end{aligned} \tag{57}$$

$$p_0^{(1)}=\frac{4-6(k-1)R^2+B_{11}(8-6R^2(k-1))}{(k-1)(-2+R^2(k-1))^2}. \tag{58}$$

We now proceed to evaluate the first order viscoelastic contribution to the hydrodynamic force and torque experienced by the spheres for the type 2 problem.

B. Hydrodynamic Force and Torque experienced by the spheres

We express the hydrodynamic force and the torque experienced by the spheres as a series expansion with Deborah number (De) as the small parameter as follows,

$$\boldsymbol{F}_i=\boldsymbol{F}_i^{(0)}+De\boldsymbol{F}_i^{(1)}+O(De^2), \tag{59}$$

$$\boldsymbol{G}_i=\boldsymbol{G}_i^{(0)}+De\boldsymbol{G}_i^{(1)}+O(De^2). \tag{60}$$

For the type 2 problem, the leading order force and torque experienced by the spheres are provided by[13] as follows,

$$\boldsymbol{F}_i^{(0)}=\boldsymbol{0}. \tag{61}$$

$$\boldsymbol{G}_1^{(0)}=-8\pi\left(\frac{P(3,(1+k)^{-1})}{(1+k)^3}-\frac{1}{2(1+k)^2}\varepsilon\log\varepsilon\right)\hat{e}_z+O(\varepsilon), \tag{62}$$

$$\boldsymbol{G}_2^{(0)}=-8\pi\left(\frac{k^3P(3,1)}{(1+k)^3}-\frac{k^3}{2(1+k)^2}\varepsilon\log\varepsilon\right)\hat{e}_z+O(\varepsilon). \tag{63}$$

Here, the function $P(a_1,b_1)$ is defined as,

$$P(a_1,b_1)=\sum_{n=0}^{\infty}(n+b_1)^{-a_1}. \tag{64}$$

We obtain the first order force and torque by substituting the velocity and pressure fields in the first order stress tensor and evaluating the surface integrals written in equations (35) and (36). The following are the obtained expressions,

$$\boldsymbol{F}_1^{(i)}=\pm\left(\frac{(1-B_{11})}{(k+1)^2}\log\varepsilon+O(\varepsilon\log\varepsilon)\right)\hat{e}_z. \tag{65}$$

$$\boldsymbol{G}_i^{(1)}=\boldsymbol{0}. \tag{66}$$

The $\pm$ sign indicates that the spheres experience equal and opposite forces. Since the value of B_{11} lies between -1 and 1, the first order viscoelastic forces experienced by the spheres are always repulsive in nature. This observation agrees with the study by Binagia and Shaqfeh[39] which noted that, a model swimmer consisting of two counter-rotating nearly touching spheres immersed in a viscoelastic fluid experiences equal and opposite forces on both the spheres. The viscoelastic force varies as $De\log\varepsilon$, which grows slowly with decreasing ε as compared to the De/ε^2 variation observed for the type 1 problem. An order of magnitude analysis reveals that only the first order pressure and the polymeric stress component contribute to the leading order viscoelastic force, and not the first order viscous stress component. Based on this analysis, the leading contribution to the vertical component of the stress tensor acting on sphere $S1$ can be written as follows,

$$\hat{e}_z\cdot\boldsymbol{T}^{(1)}\cdot\hat{e}_z=-\frac{De}{\varepsilon}\left(p_0^{(1)}+(2+B_{11})\frac{R}{H_1-H_2}\right). \tag{67}$$

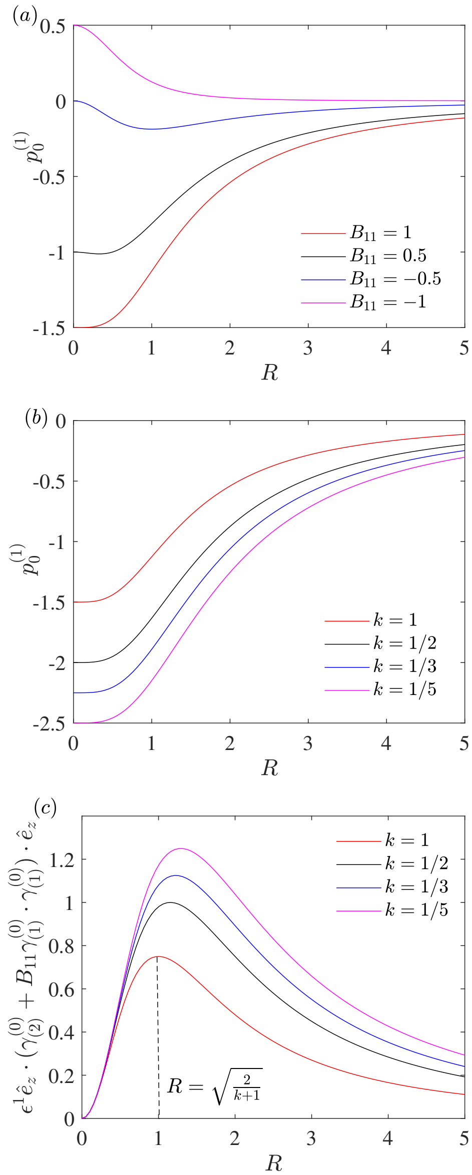

FIG. 6. a) Variation of the leading contribution to the first order pressure with the radial coordinate R for different values of B_{11}, b) Variation of the leading contribution to the first order pressure with the radial coordinate R for different values of k and c) Variation of the leading contribution to the polymeric stress component (denoted by $\boldsymbol{Q}_{zz}$ in the manuscript) with the radial coordinate R for different values of k for the type 2 problem.

From the above equation, we observe that, the first order pressure and the polymeric stress vary as ε^{-1} in the gap between the spheres and are responsible for the viscoelastic force. The first order pressure is independent of the vertical coordinate (refer to equation (58)) and is only dependent on the radial distance away from the common axis of the spheres. Figure 6a shows the variation of the first order pressure with the radial coordinate on the surface of sphere $S1$. We observe a monotonic trend for the pressure variation which is in stark contrast with the pressure variation for the type 1 problem (refer to 3a). As B_{11} varies from -1 to 1, we observe that the pressure changes sign from positive to negative. Additionally, the pressure magnitude increases with the value of B_{11} and also as the size of the sphere $S2$ is increased (refer to figures 6a and 6b). The polymeric stress in the gap between the spheres is shown in figure 6c and can be written in a simplified form as follows,

$$\boldsymbol{Q}_{zz} \sim \varepsilon^{-1}(2+B_{11})\frac{2R}{((k+1)R^2+2)^2}. \tag{68}$$

Interestingly, we note that the functional form of the polymeric stress responsible for the viscoelastic forces are similar for the type 1 and the type 2 problem (refer to equation (42)), the only difference being in the exponent of the denominator. We evaluate the radial location at which the polymeric stress is maximum to be $R = \sqrt{\frac{2}{k+1}}$.

For a sphere rotating close to a plane wall in a direction which is perpendicular to the wall, the force is obtained by substituting $k = 0$ as follows,

$$\boldsymbol{F}_{wall}^{(1)} \sim (1-B_{11})\log\varepsilon\hat{\boldsymbol{e}}_z \tag{69}$$

For the type 2 problem, reciprocal theorem was also used to determine the force acting on the spheres. This approach is outlined in detail in appendix B. However, for small sphere separations ($\varepsilon \ll 1$), the integral did not converge and hence the results are not documented in this manuscript.

IV. PROBLEM FORMULATION (TYPE 3)

Figure 7 shows a schematic representation of the type 3 problem. Sphere $S1$ rotates with an angular velocity Ω about an axis perpendicular to the line joining the centers and passing through the sphere center, while the sphere $S2$ is stationary. We use the velocity scale $u_c = \Omega a$ to non-dimensionalize the equations of motion and solve the equations in the stretches coordinates (R, Z) as defined in the previous sections. We again use a perturbation series solution with the Deborah number (De) as the small parameter and evaluate the velocity and the pressure fields in the vicinity of the spheres. As the motion of the spheres for this problem type is asymmetric, a stream function approach cannot be used and the continuity equation has to be solved explicitly. For the sake of brevity, we first provide the leading order solution here and proceed directly to the force calculation part without writing the governing equations and boundary conditions for the first order solution as the methodology remains similar to that outlined for the previous two types of problems.

A. Solution

The leading order velocity field for the type 3 problem, can be expressed in the cylindrical coordinate system as $\boldsymbol{u}^{(0)} = (U^{(0)} + O(\varepsilon), V^{(0)} + O(\varepsilon), \varepsilon^{1/2}W^{(0)} + O(\varepsilon^{3/2}))$. The expres-

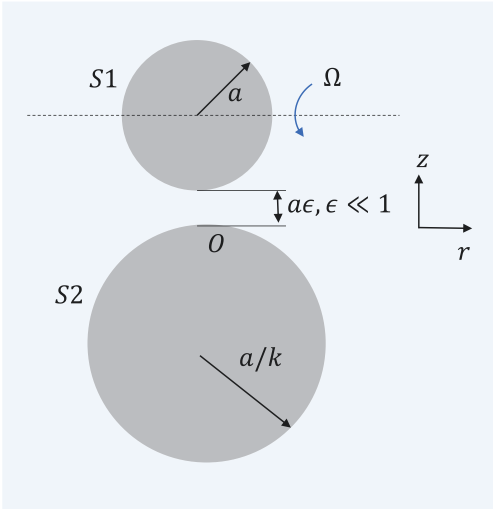

FIG. 7. Spheres immersed in a second-order fluid, with sphere $S1$ rotating with an angular velocity $\Omega\hat{e}_r$ and sphere $S2$ stationary

sions for $U^{(0)}, V^{(0)}$ are given by[14] as follows,

$$U^{(0)} = \frac{1}{5(-2+(-k-1)R^2)^3}(5k^3R^6 + k^2R^4(2+R^2+28Z) -4kR^2(-8+R^4+2Z-9Z^2-R^2(2+5Z)) + 4Z(16-2R^4-6Z+R^2(4+9Z))), \tag{70}$$

$$V^{(0)} = \frac{1}{5(-2+(-k-1)R^2)^2}(5k^2R^4 + 4Z(2+R^2+3Z) +2kR^2(2+R^2+8Z)), \tag{71}$$

The expression for $W^{(0)}$ can be derived by using the above expressions[14]. The first order solution $\boldsymbol{u}^{(1)}$ is obtained using a similar methodology as outlined in the previous sections, the derivation of which is not provided here to avoid repetition of text. Next, we solve for the force and the torque experienced by the spheres for the type 3 problem.

B. Hydrodynamic force and torque experienced by the spheres

The expressions for the leading order hydrodynamic force and torques acting on the spheres is given by O'Neill and Majumdar[10] as follows,

$$\boldsymbol{F}_1^{(0)} = \left(\frac{2}{15}\frac{1+4k}{(1+k)^2}\log\varepsilon + O(1)\right)\hat{\boldsymbol{e}}_r. \tag{72}$$

$$\boldsymbol{F}_2^{(0)} = -\left(\frac{2}{15}\frac{k^2(1+4k)}{(1+k)^2}\log\varepsilon + O(1)\right)\hat{\boldsymbol{e}}_r. \tag{73}$$

$$\boldsymbol{G}_1^{(0)} = -\left(\frac{2}{5}\frac{1}{(1+k)}\log\varepsilon + O(1)\right)\hat{\boldsymbol{e}}_r. \tag{74}$$

$$\boldsymbol{G}_2^{(0)} = \left(\frac{1}{10}\frac{k^2}{(1+k)}\log\varepsilon + O(1)\right)\hat{\boldsymbol{e}}_r. \tag{75}$$

The viscoelastic contribution to the first order force and the torque is obtained by integrating the stress tensor on the surface of the sphere using equations (35) and (36) as follows,

$$\boldsymbol{F}_1^{(1)} = -\left(\frac{28(2+B_{11})\pi}{5(1+k)\varepsilon} + O(1)\right)\hat{\boldsymbol{e}}_z. \tag{76}$$

$$\boldsymbol{F}_2^{(1)} = -\left(\frac{4(2+B_{11})\pi}{5(1+k)\varepsilon} + O(1)\right)\hat{\boldsymbol{e}}_z. \tag{77}$$

$$\boldsymbol{G}_i^{(1)} = \boldsymbol{0}. \tag{78}$$

Note that, the introduction of viscoelasticity gives rise to a lift force which is perpendicular to the direction of motion of the spheres. We also find that the lift force on sphere $S1$ acts in the negative $z-$ direction which implies that the viscoelastic lift forces on the spheres are attractive in nature. Additionally, the viscoelastic contribution to the torque acting on the spheres is zero. For sphere $S1$ rotating along an axis parallel to a plane wall, the force scales as following,

$$\boldsymbol{F}_{wall}^{(1)} \sim -\frac{28(2+B_{11})\pi}{5\varepsilon}\hat{\boldsymbol{e}}_z. \tag{79}$$

For asymmetric problems with small sphere separations, the use of reciprocal theorem to evaluate the forces acting on the spheres is computationally intractable owing to the increasing complexity of the explicit expression of the velocity field surrounding the spheres with decreasing sphere separations. For the sake of completeness, we have provided the force expression obtained using the reciprocal theorem in Appendix B for both the type 3 and type 4 problems.

V. PROBLEM FORMULATION (TYPE 4)

Figure 8 shows the schematic representation of the Type 4 problem. Sphere $S1$ is translating with a velocity U which is oriented perpendicular to the line joining the centers, while the sphere $S2$ is stationary.

A. Solution

The leading order velocity for the type 4 problem can be expressed in the cylindrical coordinate system as $\boldsymbol{u}^{(0)} = (U^{(0)} + O(\varepsilon), V^{(0)} + O(\varepsilon), \varepsilon^{1/2}W^{(0)} + O(\varepsilon^{3/2}))$. The expressions for $U^{(0)}, V^{(0)}$ are given by[14] as follows,

$$U^{(0)} = \frac{1}{5(-k-1)(-2+(-k-1)R^2)^3}(5k^4R^6 + 4Z(4+7R^4+R^2(16-9Z)+6Z) + 2k^3R^4(1+3R^2+14Z) +2k(7R^6+4(8-3Z)Z+2R^4(8+3Z)+R^2(4+52Z)) +k^2(15R^6+2R^4(23+6Z)+4R^2(8-2Z+9Z^2))), \tag{80}$$

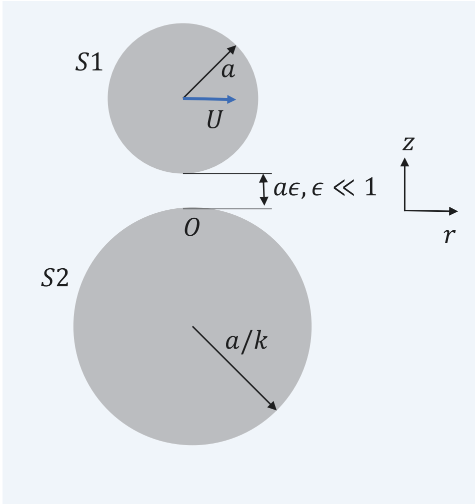

FIG. 8. Spheres immersed in a second-order fluid, with sphere $S1$ translating with a velocity $U\hat{e}_r$ and sphere $S2$ stationary

$$V^{(0)} = \frac{1}{(-k-1)5(-2+(-k-1)R^2)^2}(5k^3R^4 +4Z(8+4R^2-3Z+k^2R^2(4+7R^2+16Z) +4k(2R^4+2R^2(2+Z)+Z(2+3Z))).$$

For the sake of brevity, we now directly proceed to the force calculation without explicitly writing the solution for the first velocity velocity and pressure.

B. Hydrodynamic force and torque experienced by the spheres

The expressions for the leading order hydrodynamic force and torque acting on the spheres is given by O'Neill and Majumdar[14] as follows,

$$\boldsymbol{F}_1^{(0)} = -\left(\frac{4}{15}\frac{2+k+2k^2}{(1+k)^3}\log\varepsilon + O(1)\right)\hat{\boldsymbol{e}}_r. \quad (81)$$

$$\boldsymbol{F}_2^{(0)} = \left(|k|\frac{4}{15}\frac{2+k+2k^2}{(1+k)^3}\log\varepsilon + O(1)\right)\hat{\boldsymbol{e}}_r. \quad (82)$$

$$\boldsymbol{G}_1^{(0)} = \left(\frac{1}{10}\frac{1+4k}{(1+k)^2}\log\varepsilon + O(1)\right)\hat{\boldsymbol{e}}_r. \quad (83)$$

$$\boldsymbol{G}_2^{(0)} = -\left(|k|\frac{1}{10}\frac{4+k}{(1+k)^2}\log\varepsilon + O(1)\right)\hat{\boldsymbol{e}}_r. \quad (84)$$

The viscoelastic contribution to the first order force and the torque is obtained as follows,

$$\boldsymbol{F}_1^{(1)} = -\left(\frac{4(2+B_{11})(1+2k+7k^2)\pi}{5(1+k)^3\varepsilon} + O(1)\right)\hat{\boldsymbol{e}}_z. \quad (85)$$

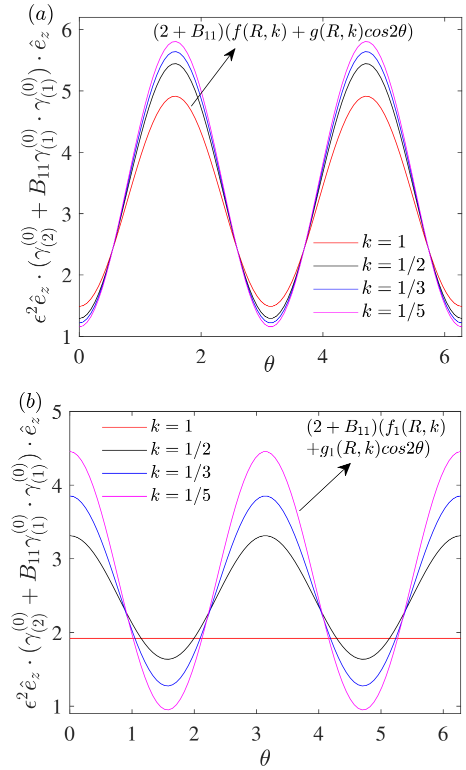

FIG. 9. Variation of the leading contribution to the polymeric stress component (denoted by $\boldsymbol{Q}_{zz}$ in the manuscript) with the azimuthal coordinate θ for different values of k for the a) type 3 problem and b) type 4 problem

$$\boldsymbol{F}_2^{(1)} = -\left(\frac{4(2+B_{11})(7+2k+k^2)\pi}{5(1+k)^3\varepsilon} + O(1)\right)\hat{\boldsymbol{e}}_z. \quad (86)$$

$$\boldsymbol{G}_i^{(1)} = \boldsymbol{0}. \quad (87)$$

We again find that the first order torque experienced by both the spheres is zero and the introduction of viscoelasticity causes the spheres to experience a lift force. The leading order viscoelastic force varies as $\sim De/\varepsilon$, which is similar to that observed for the type 3 problem. Additionally, the force acts in the negative z-direction for sphere $S1$, which signifies an attractive first order viscoelastic force. For sphere $S1$ translating parallel to a plane wall, the force scales as following,

$$\boldsymbol{F}_{wall}^{(1)} \sim -\frac{4(2+B_{11})\pi}{5\varepsilon}\hat{\boldsymbol{e}}_z. \quad (88)$$

For the type 3 and the type 4 problem, we note that only the polymeric stress contribution is responsible for the leading order viscoelastic lift forces acting on the spheres since the first order viscous stress component and the first order pressure are an order of magnitude smaller than the polymeric stress. The polymeric stress component responsible for the viscoelastic force acting on the sphere S1, for the type 3 problem can be expressed in a simplified form as follows,

$$\boldsymbol{Q}_{zz} = \varepsilon^{-2}(2+B_{11})(f(R)+g(R)\cos 2\theta). \quad (89)$$

The functional form of the above equation remains the same for the type 4 problem, with the functions $f(R), g(R)$ represented as $f_1(R), g_1(R)$. The above expression reveals that the polymeric stress varies with the azimuthal angle as $\sim \cos 2\theta$. This explains the zero first order hydrodynamic torque experienced by the sphere at this order, since $\boldsymbol{Q}_{zz}(\theta) = \boldsymbol{Q}_{zz}(\theta + \pi)$, which results in equal and opposite torques due to the polymeric stress in the two half planes canceling each other. Figures 9a and 9b show the variation of the polymeric stress with the azimuthal angle θ for the type 3 and the type 4 problems, respectively. We infer that, for both the asymmetric problem types, $\int_0^R \boldsymbol{Q}_{zz} dR > 0$ which implies that the radially averaged polymeric stress experienced by sphere $S1$ is non-zero which consequently explains the existence of a non-zero viscoelastic lift force for both type 3 and type 4 problems.

VI. CONCLUSION

In this work, we theoretically investigate the hydrodynamic forces and moments acting on two spheres which are immersed in a second-order fluid. The spheres are separated by a distance which is much smaller than the radius of either spheres. We use a regular perturbation approach with the Deborah number (De) as the small parameter in our study. The analysis presented in this manuscript is valid for weakly viscoelastic fluids with small Deborah numbers ($\sim 10^{-2} - 10^{-3}$). We show that even for weakly viscoelastic fluids, the effect of the viscoelasticity becomes important for low interparticle separations by contributing to the hydrodynamic force experienced by the particles.

We divide the problem at hand into four sub-classes, where each class is dedicated towards studying translation or rotational motion of the spheres either along the line joining the centers or the axis which is oriented perpendicular to the line joining the centers. For each of the sub-classes, we solve for the first order velocity and pressure fields in the gap between the spheres. Subsequently, we use the first order solution to obtain the viscoelastic contribution to the force and the torque experienced by the spheres. We provide the first order force and torque expressions for all the sub-classes, where the leading order contribution contains terms which are singular with respect to the sphere separation. We find that introduction of viscoelasticity does not generate any additional torque, however the viscoelastic force is non-zero and acts along the line joining the centers of both the spheres. Table IV shows the summary of the first order forces acting on the sphere for all the sub-classes. An important conclusion which can be drawn from this table is that, the magnitude of the viscoelastic force is maximum for the type 1 problem, where the force scales as De/ε^2. For the axisymmetric problems, the first order pressure and the polymeric stress are responsible for the leading order viscoelastic force acting on the spheres. The polymeric stress is maximum at a radial coordinate which is away from the common axis from the spheres and is dependent on the radius ratio of the two spheres. Both the pressure and the polymeric stress increase as the viscoelastic parameter B_{11}, which depends on the first and second normal stress coefficients, is increased. The viscoelastic force varies as De/ε^2 for spheres approaching each other and as $De\log\varepsilon$ for spheres rotating about their common axis. For asymmetric problems, only the polymeric stress is responsible for the leading order viscoelastic force acting on the spheres. The polymeric stress causes a viscoelastic lift force to act on the spheres. The lift force varies as De/ε for both the cases of spheres translating and rotating perpendicular to their common axis.

Additionally, we validate our method with the reciprocal theorem approach for the type 1 axisymmetric sub-class, and find the force estimates to be accurate for small sphere separations. For problems involving suspension of spheres in a viscoelastic fluid, the force expressions for small sphere separations are valuable due to the computational difficulties encountered in this regime. We thus propose that, the solutions provided in this manuscript be supplemented with the relevant computational technique to accurately capture the dynamics of spheres suspended in a viscoelastic fluid.

SUPPLEMENTARY MATERIAL

See the supplementary material for the complete expressions of $\psi_1^{(1)}$ and $p_1^{(1)}$.

ACKNOWLEDGMENTS

This publication was made possible due to support from NSF (grant no. 1700961). R.D. thanks Frederick N. Andrews Fellowship for financial support.

Appendix A: For Type 1 problem

Leading order solution:
The leading order solution for the stream function for the type 1 problem can be expressed as $\psi^{(0)} = \varepsilon\psi_0^{(0)} + \varepsilon^2\psi_1^{(0)} + \varepsilon^3\psi_2^{(0)} + O(\varepsilon^4)$, where $\psi_0^{(0)}, \psi_1^{(0)}$ and $\psi_2^{(0)}$ are given by,

$$\psi_0^{(0)} = A_0 Z^3 + B_0 Z^2 + C_0 Z + D_0, \tag{A1}$$

$$\psi_1^{(0)} = -\frac{1}{10} Z^5 Y A_0 - \frac{1}{6} Z^4 Y B_0 + A_1 Z^3 + B_1 Z^2 + C_1 Z + D_1, \tag{A2}$$

$$\psi_2^{(0)} = \frac{1}{280} Z^7 Y^2 A_0 + \frac{1}{120} Z^6 Y^2 B_0 - \frac{1}{10} Z^5 (Y A_1 + \frac{1}{12} Y^2 C_0) - \frac{1}{6} Z^4 (Y B_1 + \frac{1}{4} Y^2 D_0) + A_2 Z^3 + B_2 Z^2 + C_2 Z + D_2. \tag{A3}$$

Here $A_0, B_0, C_0, D_0, A_1, B_1, C_1, D_1, A_2, B_2, C_2, D_2$ are functions of R and Z, the detailed form of which is provided in Jeffrey[13] and the operator Y is defined as $\frac{\partial^2}{\partial R^2} - \frac{1}{R}\frac{\partial}{\partial R}$.

Application of reciprocal theorem to find the first order force:

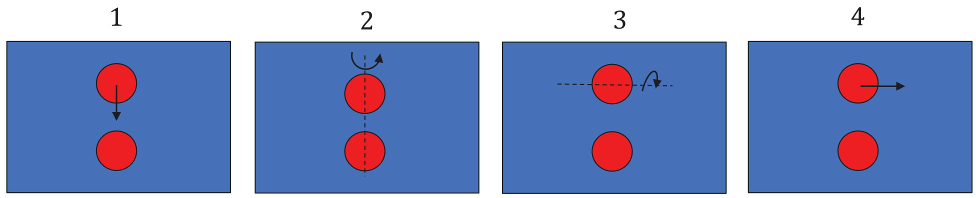

Type	Viscoelastic force		Direction	Sphere $S1$ near wall
	Sphere $S1$	Sphere $S2$		
1	$\frac{3De\pi(8+3B_{11})}{5(1+k)^2\varepsilon^2}$	$\frac{3De\pi(8+3B_{11})}{5(1+k)^2\varepsilon^2}$	Repulsive	$\frac{3De\pi(8+3B_{11})}{5\varepsilon^2}$
2	$\frac{(1-B_{11})}{(1+k)^2}De\log\varepsilon$	$\frac{(1-B_{11})}{(1+k)^2}De\log\varepsilon$	Repulsive	$(1-B_{11})De\log\varepsilon$
3	$-\frac{28De(2+B_{11})\pi}{5(1+k)\varepsilon}$	$-\frac{4De(2+B_{11})\pi}{5(1+k)\varepsilon}$	Attractive	$-\frac{28De(2+B_{11})\pi}{5\varepsilon}$
4	$-\frac{4De(2+B_{11})(1+2k+7k^2)\pi}{5(1+k)^3\varepsilon}$	$-\frac{4De(2+B_{11})(7+2k+k^2)\pi}{5(1+k)^3\varepsilon}$	Attractive	$-\frac{4De(2+B_{11})\pi}{5\varepsilon}$

TABLE IV. Viscoelastic contribution to the force acting on the spheres immersed in a second- order fluid along with their direction. Note that the force acts along the line joining the sphere centers.

For applying the reciprocal theorem, we define the auxillary problem to be that of the sphere $S1$ approaching the stationary sphere $S2$ with a unit velocity. We define the corresponding stress field and velocity fields by $\boldsymbol{S}^*, \boldsymbol{v}^*$, respectively. We begin by writing the following equation which uses the divergence free property of the stress tensors $\boldsymbol{T}^{(1)}$ and $\boldsymbol{S}^*$,

$$\int_{V_f}\left(\boldsymbol{v}^*\cdot(\boldsymbol{\nabla}\cdot\boldsymbol{T}^{(1)})-\boldsymbol{u}^{(1)}\cdot(\boldsymbol{\nabla}\cdot\boldsymbol{S}^*)\right)dV=0, \tag{A4}$$

Consequently, we can write the following,

$$\int_{V_f}\boldsymbol{\nabla}\cdot\left(\boldsymbol{v}^*\cdot\boldsymbol{T}^{(1)}-\boldsymbol{u}^{(1)}\cdot\boldsymbol{S}^*\right)dV = \int_{V_f}\left(\boldsymbol{T}^{(1)}:\boldsymbol{\nabla}\boldsymbol{v}^*-\boldsymbol{S}^*:\boldsymbol{\nabla}\boldsymbol{u}^{(1)}\right)dV, \tag{A5}$$

We now use the divergence theorem to convert the volume integral on the left to a surface integral and use the boundary conditions on the sphere surfaces as well the definition of the surface stress tensor $\boldsymbol{T}^{(1)}$(refer to equation (8)) to obtain the force acting on the sphere $S1$ as follows,

$$\boldsymbol{F}_1=\int_{V_f}\left(\dot{\gamma}^{(0)}_{(2)}+B_{11}\dot{\gamma}^{(0)}_{(1)}\cdot\dot{\gamma}^{(0)}_{(1)}\right):\boldsymbol{\nabla}\boldsymbol{u}^{(0)}\hat{\boldsymbol{e}}_z. \tag{A6}$$

For the type 1 problem, we evaluate the above expression by substituting the velocity field obtained for sphere $S1$ translating towards a stationary sphere $S2$, with both the spheres immersed in a Newtonian fluid[7].

Appendix B: For Type 2,3,4 problems

Application of reciprocal theorem to find the first order force:

For applying the reciprocal theorem for the type 2,3 and 4 problems, we choose the auxillary problem to be that of sphere $S1$ translating with a velocity of $-\hat{\boldsymbol{e}}_z$ and sphere $S2$ stationary. The solution of this problem is given by Brenner[7] and is denoted by $\boldsymbol{u}^{(0)}$. After applying the reciprocal theorem, we obtain the following expression for the force acting on the sphere $S1$,

$$\boldsymbol{F}_1=\int_{V_f}\left(\dot{\gamma}^{(0)}_{(2)}+B_{11}\dot{\gamma}^{(0)}_{(1)}\cdot\dot{\gamma}^{(0)}_{(1)}\right):\boldsymbol{\nabla}\boldsymbol{u}^{(0)}\hat{\boldsymbol{e}}_z. \tag{B1}$$

Here, the expression inside the round brackets is evaluated by substituting the relevant solutions for sphere $S1$ immersed in a Newtonian fluid and rotating with an angular velocity of $\hat{\boldsymbol{e}}_z$, rotating with an angular velocity of $\hat{\boldsymbol{e}}_r$ and translating with a linear velocity of $\hat{\boldsymbol{e}}_r$ for type 2, 3 and 4 problems, respectively[15,49].

DATA AVAILABILITY STATEMENT

The data that supports the findings of this study are available within the article.

[1] L. Leal, "Particle motions in a viscous fluid," Annu. Rev. Fluid Mech. **12**, 435–476 (1980).
[2] A. Karimi, S. Yazdi, and A. Ardekani, "Hydrodynamic mechanisms of cell and particle trapping in microfluidics," Biomicrofluidics **7**, 021501 (2013).
[3] H. A. Stone, A. D. Stroock, and A. Ajdari, "Engineering flows in small devices: microfluidics toward a lab-on-a-chip," Annu. Rev. Fluid Mech. **36**, 381–411 (2004).
[4] D. Di Carlo, D. Irimia, R. G. Tompkins, and M. Toner, "Continuous inertial focusing, ordering, and separation of particles in microchannels," Proc. Natl. Acad. Sci. **104**, 18892–18897 (2007).
[5] A. Raffiee, A. Ardekani, and S. Dabiri, "Numerical investigation of elasto-inertial particle focusing patterns in viscoelastic microfluidic devices," J Nonnewton Fluid Mech **272**, 104166 (2019).
[6] M. Stimson and G. Jeffery, "The motion of two spheres in a viscous fluid," Proc. R. Soc. Lond. **111**, 110–116 (1926).
[7] H. Brenner, "The slow motion of a sphere through a viscous fluid towards a plane surface," Chem.Eng.Sci. **16**, 242–251 (1961).
[8] A. Maude, "End effects in a falling-sphere viscometer," Br. J. Appl. Phys. **12**, 293 (1961).
[9] G. Jeffery, "On the steady rotation of a solid of revolution in a viscous fluid," PLMS **2**, 327–338 (1915).

[10]M. O'Neill and S. Majumdar, "Asymmetrical slow viscous fluid motions caused by the translation or rotation of two spheres. part i: The determination of exact solutions for any values of the ratio of radii and separation parameters," Zeitschrift für angewandte Mathematik und Physik ZAMP **21**, 164–179 (1970).

[11]M. Cooley and M. O'Neill, "On the slow motion generated in a viscous fluid by the approach of a sphere to a plane wall or stationary sphere," Mathematika **16**, 37–49 (1969).

[12]R. Hansford, "On converging solid spheres in a highly viscous fluid," Mathematika **17**, 250–254 (1970).

[13]D. Jeffrey, "Low-reynolds-number flow between converging spheres," Mathematika **29**, 58–66 (1982).

[14]M. O'Neill and S. Majumdar, "Asymmetrical slow viscous fluid motions caused by the translation or rotation of two spheres. part ii: Asymptotic forms of the solutions when the minimum clearance between the spheres approaches zero," Zeitschrift für angewandte Mathematik und Physik ZAMP **21**, 180–187 (1970).

[15]D. Jeffrey and Y. Onishi, "The forces and couples acting on two nearly touching spheres in low-reynolds-number flow," Zeitschrift für angewandte Mathematik und Physik ZAMP **35**, 634–641 (1984).

[16]F. M. Leslie and R. I. Tanner, "The slow flow of a visco-elastic liquid past a sphere," Q. J. Mech. Appl. Math. **14**, 36–48 (1961).

[17]B. Caswell and W. H. Schwarz, "The creeping motion of a non-newtonian fluid past a sphere," J.Fluid.Mech. **13**, 417–426 (1962).

[18]M. D. Chilcott and J. M. Rallison, "Creeping flow of dilute polymer solutions past cylinders and spheres," J .Nonnewton .Fluid .Mech **29**, 381–432 (1988).

[19]B. Caswell, "The effect of finite boundaries on the motion of particles in non-newtonian fluids," Chem.Eng.Sci. **25**, 1167–1176 (1970).

[20]B. Caswell, "The stability of particle motion near a wall in newtonian and non-newtonian fluids," Chem.Eng.Sci. **27**, 373–389 (1972).

[21]B. Ho and L. Leal, "Migration of rigid spheres in a two-dimensional unidirectional shear flow of a second-order fluid," J.Fluid.Mech, **76**, 783–799 (1976).

[22]L. E. Becker, G. H. McKinley, and H. A. Stone, "Sedimentation of a sphere near a plane wall: weak non-newtonian and inertial effects," J .Nonnewton .Fluid .Mech **63**, 201–233 (1996).

[23]J. Feng, P. Huang, and D. Joseph, "Dynamic simulation of sedimentation of solid particles in an oldroyd-b fluid," J.Non-Newton.Fluid. **63**, 63–88 (1996).

[24]P. Singh and D. Joseph, "Sedimentation of a sphere near a vertical wall in an oldroyd-b fluid," J.Non-Newton.Fluid. **94**, 179–203 (2000).

[25]A. Ardekani, R. Rangel, and D. Joseph, "Motion of a sphere normal to a wall in a second-order fluid," J.Fluid.Mech. **587**, 163–172 (2007).

[26]P. Brunn, "Interaction of spheres in a viscoelastic fluid," Rheol.Acta **16**, 461–475 (1977).

[27]A. Ardekani, R. Rangel, and D. Joseph, "Two spheres in a free stream of a second-order fluid," Phys. Fluids **20**, 063101 (2008).

[28]R. Phillips, "Dynamic simulation of hydrodynamically interacting spheres in a quiescent second-order fluid," J.Fluid.Mech. **315**, 345–365 (1996).

[29]A. Khair and T. Squires, "Active microrheology: a proposed technique to measure normal stress coefficients of complex fluids," Phys.Rev.Lett. **105**, 156001 (2010).

[30]A. Vázquez-Quesada and M. Ellero, "Analytical solution for the lubrication force between two spheres in a bi-viscous fluid," Phys.Fluids **28**, 073101 (2016).

[31]A. Vázquez-Quesada, N. J. Wagner, and M. Ellero, "Normal lubrication force between spherical particles immersed in a shear-thickening fluid," Phys.Fluids **30**, 123102 (2018).

[32]R. Tanner, "A short-bearing solution for pressure distribution in a non-newtonian lubricant," J. Appl. Mech-T. ASME. (1964).

[33]Y. Hsu, "Non-newtonian flow in infinite-length full journal bearing," J. Lubr. Technol-T. ASME. (1967).

[34]S. Wada and H. Hayashi, "Hydrodynamic lubrication of journal bearings by pseudo-plastic lubricants: part 1, theoretical studies," Bull.JSME. **14**, 268–278 (1971).

[35]J. Tichy, "Non-newtonian lubrication with the convected maxwell model," J. Trib. (1996).

[36]F. T. Akyildiz and H. Bellout, "Viscoelastic lubrication with phan-thein-tanner fluid (ptt)," J. Trib. **126**, 288–291 (2004).

[37]D. Gwynllyw and T. Phillips, "The influence of oldroyd-b and ptt lubricants on moving journal bearing systems," J.Non-Newton.Fluid. **150**, 196–210 (2008).

[38]A. Abbaspur, M. Norouzi, P. Akbarzadeh, and S. A. Vaziri, "Analysis of nonlinear viscoelastic lubrication using giesekus constitutive equation," Proc. Inst. Mech. Eng. J , 1350650120944280 (2020).

[39]J. P. Binagia and E. S. Shaqfeh, "Self-propulsion of a freely suspended swimmer by a swirling tail in a viscoelastic fluid," Phys.Rev.Fluids **6**, 053301 (2021).

[40]J. A. PPuente-Velázquez, F. A. Godínez, E. Lauga, and R. Zenit, "Viscoelastic propulsion of a rotating dumbbell," Microfluid. Nanofluidics **23**, 1–7 (2019).

[41]O. S. Pak, L. Zhu, L.and Brandt, and E. Lauga, "Micropropulsion and microrheology in complex fluids via symmetry breaking," Phys.Fluids **24**, 103102 (2012).

[42]M. Yang and E. S. Shaqfeh, "Mechanism of shear thickening in suspensions of rigid spheres in boger fluids. part i: Dilute suspensions," J.Rheol **62**, 1363–1377 (2018).

[43]M. Yang and E. S. Shaqfeh, "Mechanism of shear thickening in suspensions of rigid spheres in boger fluids. part ii: Suspensions at finite concentration," J.Rheol **62**, 1379–1396 (2018).

[44]D. Alghalibi, L. Lashgari, I.and Brandt, and S. Hormozi, "Interface-resolved simulations of particle suspensions in newtonian, shear thinning and shear thickening carrier fluids," J.Fluid.Mech. **852**, 329–357 (2018).

[45]A. Vázquez-Quesada, P. Español, R. I. Tanner, and M. Ellero, "Shear thickening of a non-colloidal suspension with a viscoelastic matrix," Journal of Fluid Mechanics **880**, 1070–1094 (2019).

[46]G. D'Avino, F. Greco, M. A. Hulsen, and P. L. Maffettone, "Rheology of viscoelastic suspensions of spheres under small and large amplitude oscillatory shear by numerical simulations," J.Rheol. **57**, 813–839 (2013).

[47]R. B. Bird, R. C. Armstrong, and O. Hassager, "Dynamics of polymeric liquids. vol. 1: Fluid mechanics," (1987).

[48]H. Masoud and H. Stone, "The reciprocal theorem in fluid dynamics and transport phenomena," J.Fluid.Mech. **879** (2019).

[49]A. J. Goldman, R. G. Cox, and H. Brenner, "The slow motion of two identical arbitrarily oriented spheres through a viscous fluid," Chem.Eng.Sci. **21**, 1151–1170 (1966).